Lawrence Berkeley Laboratory
UNIVERSITY OF CALIFORNIA

Materials & Chemical Sciences Division

Presented at the Workshop on Competing Interactions and Microstructures: Statics and Dynamics, Los Alamos, NM, May 5–8, 1987, and to be published in the Proceedings

Cu_3Pd Observed by High-Voltage Electron Microscopy

J. Kulik, S. Takeda, and D. de Fontaine

July 1987

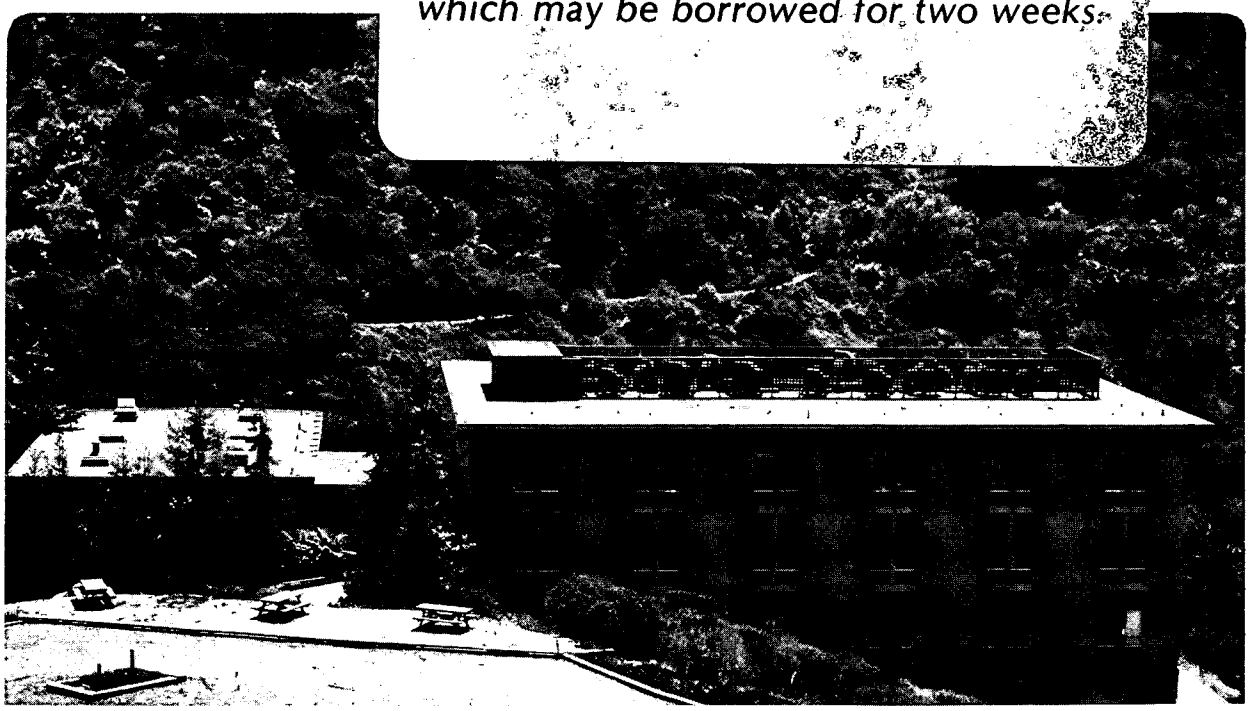

Prepared for the U.S. Department of Energy under Contract DE-AC03-76SF00098

DISCLAIMER

LBL-23757

Cu_3Pd Observed by High-Voltage Electron Microscopy

J. Kulik, S. Takeda*, and D. de Fontaine

Materials and Chemical Sciences Division
Lawrence Berkeley Laboratory
University of California
Berkeley, CA 94720

*Permanent Address: College of Education,
Osaka University, 1-1 Machikaneyama-cho,
Toyonaka-shi, Osaka, 560, JAPAN

July 1987

This work was supported by the Director, Office of Energy Research, Office of Basic Energy Sciences, Materials Sciences Division of the U.S. Department of Energy under Contract No. DE-AC03-76SF00098.

Cu_3Pd Observed by High-Voltage Electron Microscopy

by

J. Kulik, S. Takeda* and D. de Fontaine

Materials and Chemical Sciences Division, Lawrence Berkeley Laboratory, Berkeley, CA 94720

**Permanent address: College of Education, Osaka University, 1-1 Machikaneyama-cho, Toyonaka-shi, Osaka 560, JAPAN*

Abstract

Cu-Pd samples of compositions varying from 16 to 26 at.% Pd were irradiated *in situ* in a 1.5 MeV electron microscope at various temperatures. Low temperature (90 K) irradiation produced completely disordered solid solutions. Irradiation at room temperature up to as high as about 500 K produced steady state short range order (SRO) which, for specimens of 18% or more Pd, is characterized by diffuse intensity at $[1,\pm q,0]$ and equivalent positions in reciprocal space (modulated SRO). In general, q is a function of composition, temperature and irradiation dose. High temperature irradiation tended to produce the expected equilibrium long range order — either $L1_2$ or a long period superstructure depending on composition and temperature. The 18 and 20% samples irradiated at room temperature exhibited steady state *modulated* SRO even though the expected equilibrium structure is one of *unmodulated* order ($L1_2$). It is suggested that spinodal ordering is responsible for this latter effect. An f.c.c.-based Cu-Pd phase diagram is proposed incorporating ordering stability loci and a metastable Lifshitz point.

1. Introduction

It is well known that, below about 800 K, Cu-Pd f.c.c. solid solutions undergo ordering reactions in the range of about 10 to 30 at.% Pd. Evidence has come from x-ray diffraction [1-5], and electron diffraction and microscopy [5-9]. From these and other data, SUBRAMANIAN and LAUGHLIN [10] proposed an assessed phase diagram of which Fig. 1 is a slightly modified version. The modifications were introduced in order to attempt to incorporate the very recent results of BRODDIN *et al.*[11]. The heavy solid lines in the figure indicate equilibria between the f.c.c. solid solution (α) and the f.c.c.-derived ordered phases. Much of this diagram is of speculative nature as no firm evidence for the peritectoid reactions exist. Nevertheless, certain basic features are well established. The phase region (α') of the simple ordered structure $L1_2$ (Cu_3Au type) peaks not at the expected stoichiometric composition of 25%, but at around 15% Pd. Near stoichiometry, one-dimensional long-period superstructures (LPS) (α_1 region) are found, being replaced at higher Pd content by two-dimensional LPS (α_2 region). At still higher Pd content, a (B2) b.c.c. superstructure (β') becomes stable. Stable B2-related equilibria are indicated by light lines in Fig. 1. The dashed lines are *ordering spinodals*, to be discussed later. The two open circles shown on the diagram indicate the presence of one-dimensional LPS according to BRODDIN *et al.* [11]. Clearly, in that region, the one-dimensional LPS may well be metastable with respect to the two-dimensional LPS, and both one- and two-dimensional LPS are certainly metastable with respect to the stable $\alpha_2 + \beta'$ equilibrium.

Recently, there has been a resumption of interest in alloys with LPS since it was suggested [12-16] that generalizations of the so-called axial next nearest neighbor Ising (ANNNI) model could serve as simple theoretical paradigms for these systems. The original explanation for the stability of LPS, based on Fermi surface considerations [17], is certainly still considered valid, especially now that GYORFFY and STOCKS [18] have given the idea a firmer quantitative basis. Nevertheless, viewing these alloys as Ising systems with competing interactions has proven to be a useful approach. Polytypes encountered in Ag_3Mg [16] and Al_3Ti [14], for example, agree well with ANNNI model predictions.

The experimental Cu-Pd phase diagram certainly merits further study. However, kinetics in this system are extremely sluggish and virtually nonexistent near room temperature. Consequently, statements concerning equilibrium configurations at these temperature must be made with

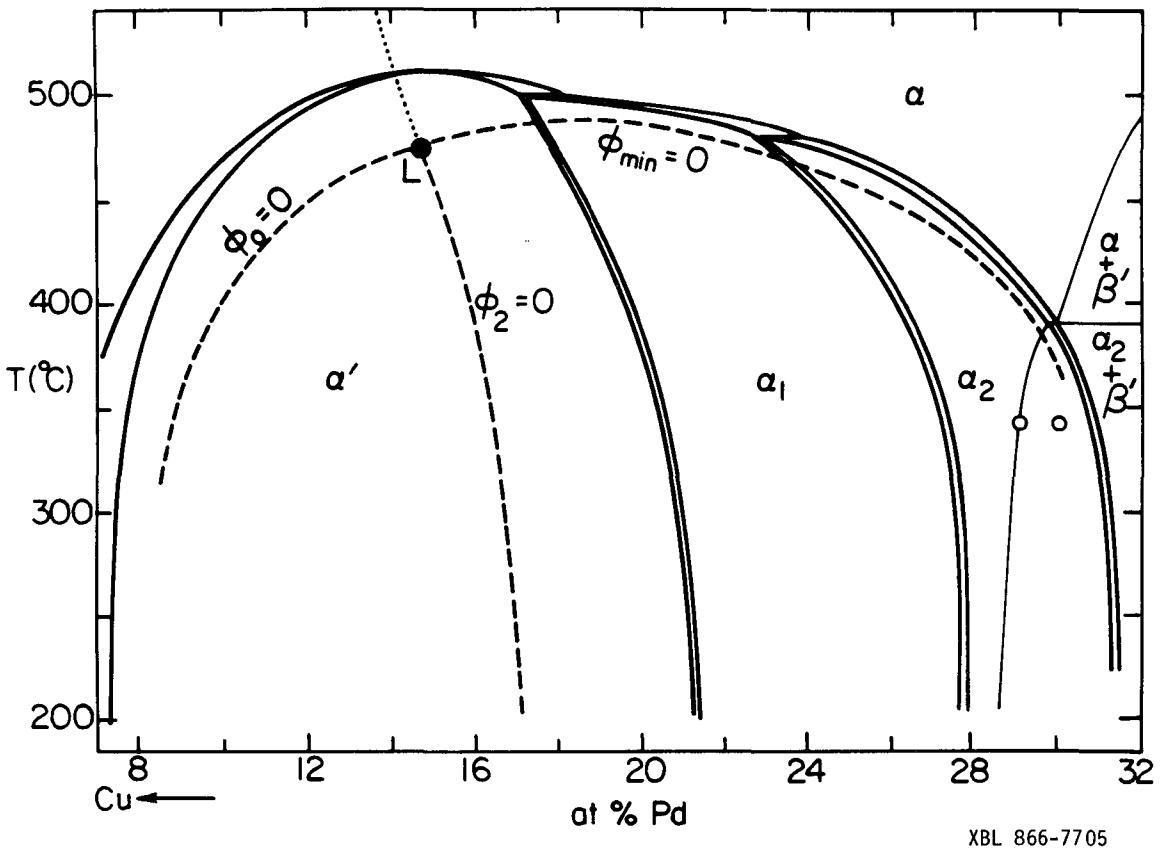

Fig. 1. Cu rich side of the Cu-Pd phase diagram

caution and are difficult to verify. In an attempt to increase the rate of kinetic processes we performed *in situ* irradiation of several Cu-Pd specimens in a 1.5 MeV transmission electron microscope (TEM).

In general, irradiation of metals by high energy electrons results in a number of different processes including the replacement and displacement of atoms. There is a consequent increase in the concentration of vacancies and interstitials. In long range ordered (LRO) or short range ordered (SRO) alloys, destruction of order may result at sufficiently low temperatures. On the other hand, ordering during irradiation can occur if the temperature is sufficiently high to allow the thermal motion of the irradiation-induced point defects. (A summary of these effects can be found in URBAN, BANERJEE and MAYER [19] and references cited therein.) In the case of Cu-Pd, it was hoped that the excess vacancies induced by the high energy electron beam would enhance the ordering kinetics at room temperature. However, instead of obtaining a long range ordered state, modulated short range order was obtained, even in regions where an *unmodulated* long range ordered structure (i.e., $L1_2$) was the expected equilibrium state. By "modulated short range order" we mean the presence in diffraction data of broad, diffuse peaks of intensity located away from one of the special points of high symmetry in the Brillouin zone. The displacement of the peaks from the special point is the modulation wave vector. This is discussed further in Section 3 below. The unexpected occurrence of this SRO state has revealed something of the nature of the thermodynamic instabilities which underlie the first order transitions occurring in this system. We present in this paper a description of this result.

2. Experimental Results

Alloys of 16, 18, 20, 22, and 26 at.% Pd were prepared by arc-melting under an Ar atmosphere. The ingots were held just below the melting point for several hours. Pieces of the original ingots were then remelted and splat cooled through the courtesy of L. E. Tanner at Lawrence Livermore Laboratory. The purpose of the splat cooling was to obtain a pronounced <100> texture. The

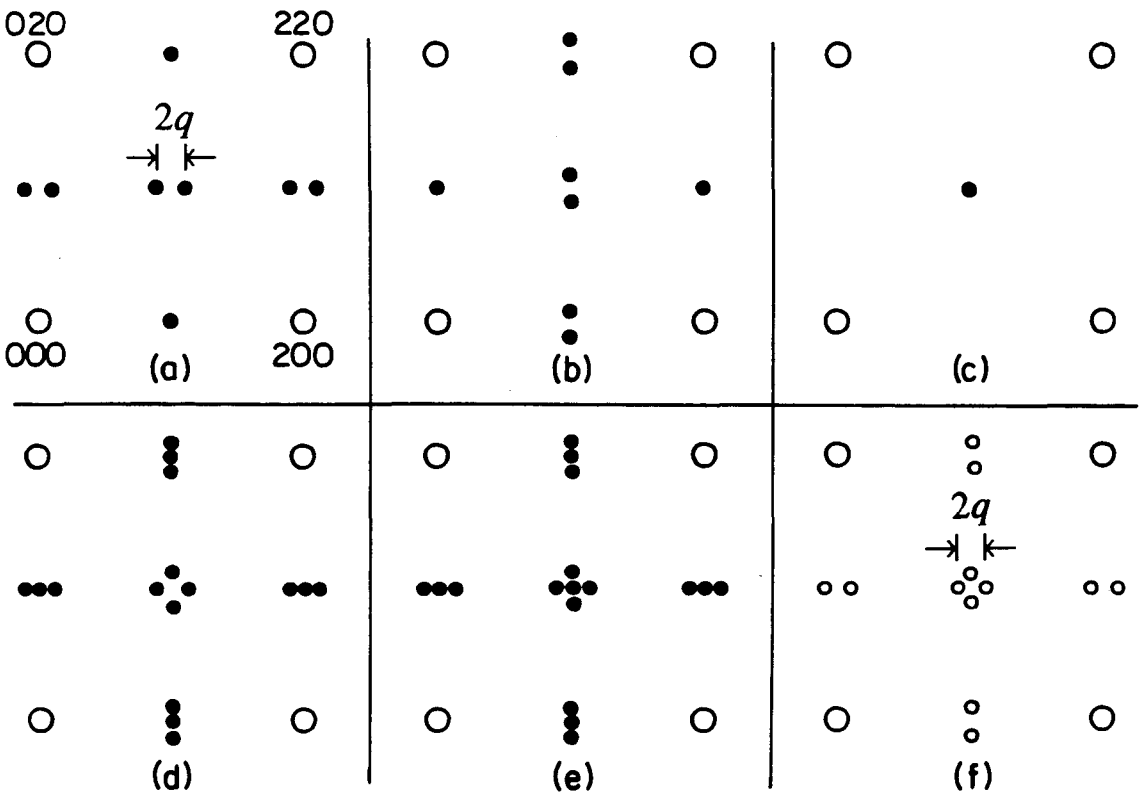

Fig. 2. Schematic of diffraction patterns from the one-dimensional LPS and from the SRO state

XBL 866-7706

splat cooled foils were then homogenized in sealed quartz tubes at 1270 K under one atmosphere of Ar for one day. Solutionized foils were quenched in ice water. Disks for TEM observation were punched and electrolytically polished in a methanol solution of 15% HNO_3 at about -60° C.

After being quenched, the specimens were observed in a conventional TEM (100 kV) and then transferred to the 1.5 MeV machine at the National Center for Electron Microscopy at Lawrence Berkeley Laboratory. Use of both low and high temperature double tilting stages provided a temperature range of about 90 K to over 770 K. Diffraction patterns of all samples were taken of the as-quenched samples in the [100] orientation. For some specimens, electron irradiation was then performed at 90 K at which temperature all traces of SRO are destroyed. Subsequent evolution of the disordered regions under irradiation at room temperature could then be followed *in situ*. In addition the heating stage was used to perform *in situ* irradiation at temperatures from about 470 K up to the disordering temperature.

In what follows, all temperatures cited are those of the thermocouple on the specimen stage of the microscope. The actual temperatures of the irradiated areas were certainly higher, perhaps by a few tens of degrees.

The most extensive observations were made on the 20% Pd specimen. We begin with a description of these results. As a convenient reference, Fig. 2 is a schematic of electron diffraction patterns in [001] incidence from modulated LRO and modulated SRO specimens. Patterns (a), (b) and (c) show the three possible variants of the one-dimensional LPS which are, respectively, modulation along [100], [010] and [001]. Pattern (d) is a combination of (a) and (b), while (e) is a combination of all three variants. Pattern (f) is indicative of SRO. The small open circles in (f) are meant to indicate diffuse peaks as opposed to the sharp superstructure peaks in the LRO patterns. Note the absence of intensity at [100] and equivalent positions in (f). In all cases, the modulation can be characterized by the separation $2q$ of the satellite pairs. The quantity q is then the distance of the peaks from the [100] (or equivalent) position; that is, q is

the modulation wave number. In contrast, Fig. 11 shows an example where the SRO or LRO peaks occur *at* the special point (i.e., [100] and equivalent).

Figure 3(a) is an *in situ* high temperature pattern. It is clearly indicative of SRO fluctuations above the transition temperature. The long wavelength modulation characteristic of the SRO fluctuations in this alloy is in agreement with earlier observation [20, 21]. The diffraction pattern of the specimen as quenched from 1270 K is shown in Fig. 3(b). At 1270 K no SRO fluctuations are expected to be observable. The fact that they are present in the quenched specimen indicates that a certain amount of spinodal ordering (to be discussed later) has occurred during the quench. The intensity pattern of Fig. 3(b) is similar in character to that of Fig. 3(a) but with an increase in amplitude and sharpening of the satellites flanking the [100] (and equivalent) positions.

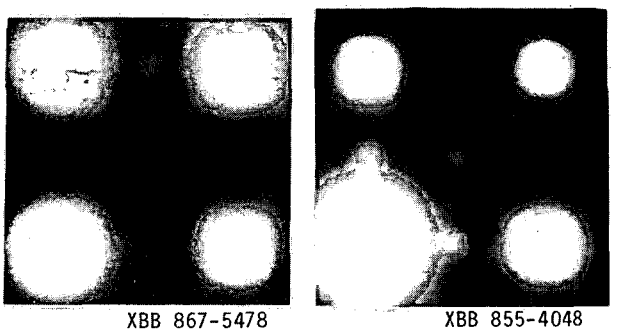

Fig. 3. Cu 20% Pd: (a) equilibrium fluctuations *in situ* at 810 K, (b) as quenched from 1270 K

Irradiation of the as-quenched specimen at room temperature does *not* produce the long range ordered structure which, according to the phase diagram of Fig. 1, is the $L1_2$. Rather, the state depicted in Fig. 3(b) essentially persists with a slight increase in satellite intensity and a small decrease in the value of q. This persistence of SRO is typical of all of our specimens at room temperature. The specimens of 18, 20, 22, and 26% Pd all displayed diffuse satellites around the [100] position. The 16% Pd specimen displayed diffuse scattering *at* the [100] position but, at room temperature, the intensity never became sharp enough to allow the structure to be characterized as long range ordered. These results are in contrast to a previous HVEM study in which a 25% Pd specimen was irradiated at room temperature to produce the long range ordered one-dimensional superstructure [22]. The difference between that experiment and the present one is in the energy of the electrons and the electron dose rate. Our experiment employed higher energy electrons (1.5 MeV as compared with 1 MeV) and a higher flux rate (an estimated 10^{21} electrons per cm^2 per second as compared with 2×10^{19} electrons per cm^2 per second).

In situ irradiation at 90 K completely destroys the short range order as seen in Fig. 4(a). This effect is similar to that observed previously in Ni_4Mo by other investigators [22-25]. At this temperature, the high energy electrons are inducing disorder through several different mechanisms including replacement collision sequences and random point-defect annihilation. The latter process is enhanced by the supersaturation of vacancies. Despite this supersaturation, the mobility of the vacancies is quite low at this temperature, and the *reordering* mechanism is effectively frozen.

When the temperature is increased to 290 K and irradiation resumed, the modulated SRO state reappears as seen in Figs. 4(b) through 4(c). Thus, despite an initial condition of *complete* disorder, the system still evolves toward a SRO state rather than the expected $L1_2$ equilibrium. As in the previous example, where irradiation was begun with the SRO state already present, continued irradiation does not promote LRO but causes some sharpening of and increase in intensity of the satellites accompanied by a small increase in the modulation wavelength, i.e., the satellites move toward the [100] position. The plot of Fig. 5 shows the modulation wave vector vs. time for the specimen irradiated at room temperature. There is also some indication that the value of

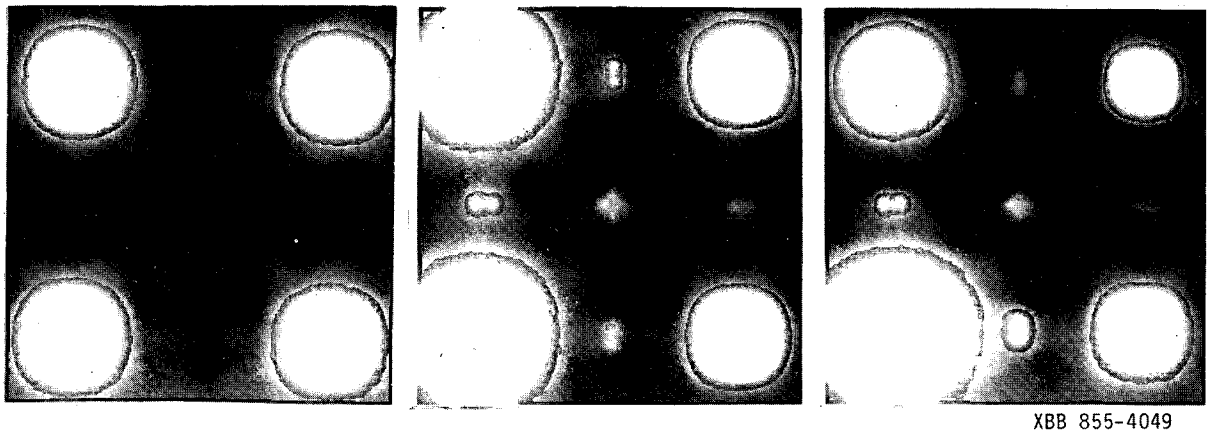

Fig. 4. Cu 20% Pd: (a) after irradiation at 90 K, (b) after 185 s of irradiation at room temperature, (c) after 720 s of irradiation

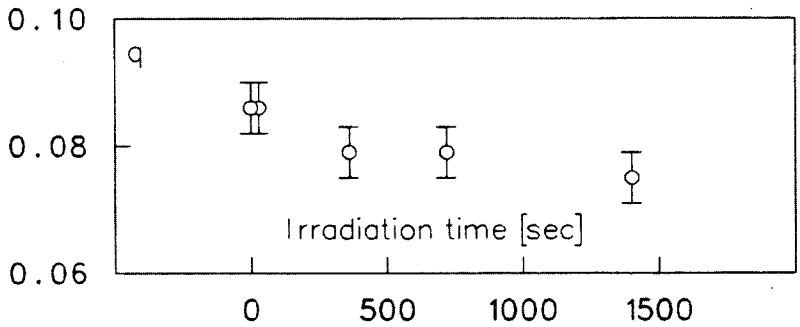

Fig. 5. Cu 20% Pd: wave number q as a function of irradiation time in the SRO state at room temperature

q at which intensity initially appears depends on temperature. A disordered specimen irradiated at 170 K exhibits an initial appearance of intensity at $q = 0.05 \pm 0.01$ as compared with an initial q of about 0.085 at 290 K as shown in Fig. 5.

Irradiation at 620 K produces what appears to be a mixed state. After irradiation at 90 K the specimen was heated to 620 K where weak SRO appears even before irradiation is begun (Fig. 6(a)). Irradiation causes a dramatic increase in the intensity and sharpness of the satellites after only 10 s (Fig. 6(b)). After prolonged irradiation intensity appears at the [100] position indicating that some LRO must be present (Fig. 6(c)). Weak SRO continues to coexist with the LRO long-period superstructure, however. This is seen most readily at higher diffracting angles where the film has not been saturated by the superlattice reflections. Figure 7 shows the intensity pattern around the [300] position. Notice that the diffuse intensity does not lie on the line determined by the sharp satellite reflections arising from the LRO. This is due to the tetragonality of the LRO phase. The broad streaking of the SRO scattering makes determination of its modulation wavelength impractical. Figure 8 shows the modulation wave vector vs. time. The onset of LRO is also indicated.

Irradiation at higher temperatures rapidly results in the formation of the LRO one-dimensional LPS. Figure 9 shows the evolution in time of the diffraction pattern. The initial state already exhibits intensity peaks since the temperature is sufficiently high to allow the occurrence of normal kinetics. These peaks are quite sharp (discouraging their characterization as SRO) although no peaks are present at [100] or equivalent positions. After 30 s of irradiation,

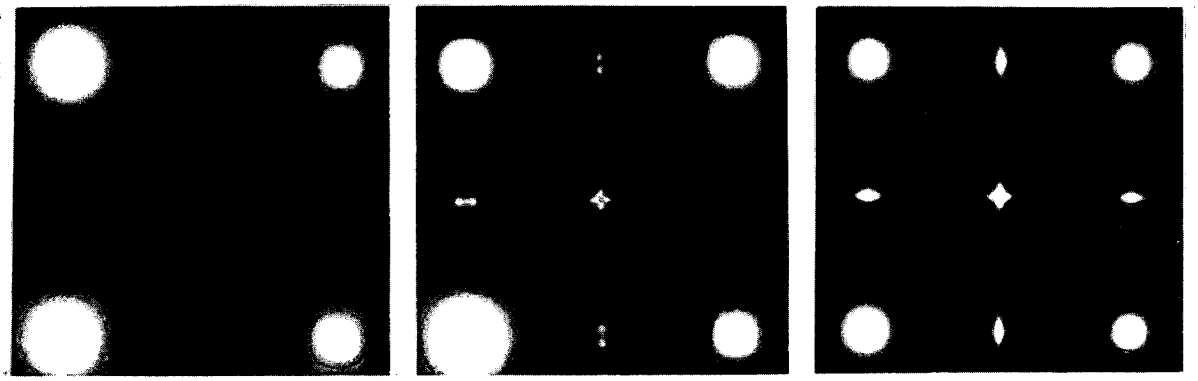

XBB 855-4052

(a) (b) (c)

Fig. 6. Cu 20% Pd at 620 K: (a) weak SRO, (b) after 10 s of irradiation, (c) after 1440 s of irradiation

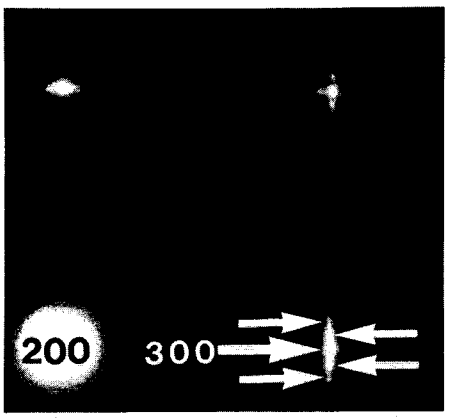

XBB 873-1992

Fig. 7. Intensity surrounding the [300] position in Cu 20% Pd irradiated for 1440 s at 620 K

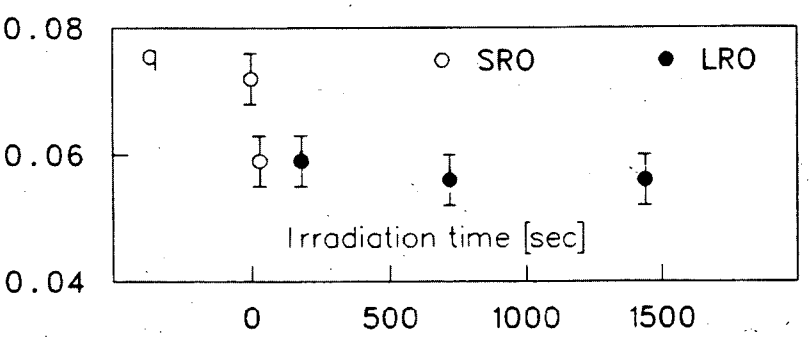

Fig. 8. Cu 20% Pd at 620 K: wave number q as a function of irradiation time

intensity appears at [100], indicative of the normal one-dimensional LPS, accompanied by a decrease in the modulation wavelength (i.e., movement of the satellites away from [100]). This is in contrast to the behavior of irradiated SRO at lower temperatures where the modulation wavelength *increases*. The change of wave vector vs. time is shown in Fig. 10.

Next, let us turn our attention to the 16% Pd specimen. In both the *in situ* high temperature diffraction pattern and the as-quenched pattern no splitting or departure from spherical symmetry

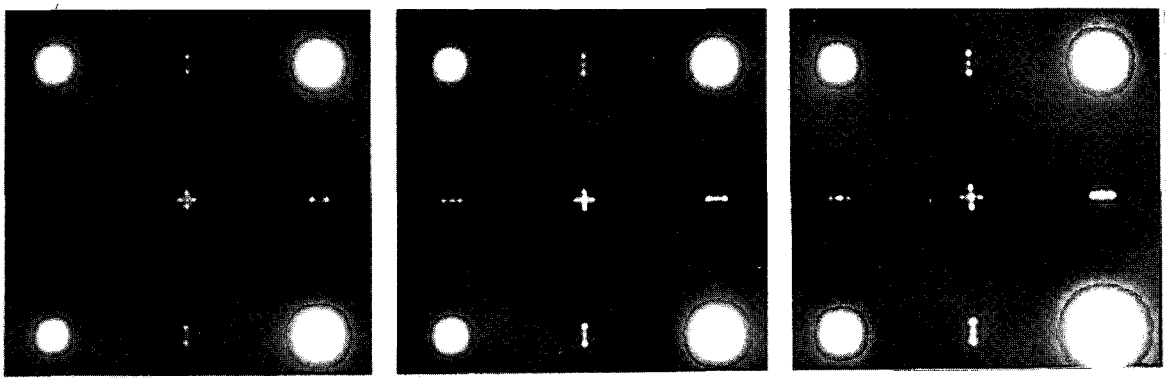

XBB 855-4051

(a) (b) (c)

Fig. 9. Cu 20% Pd at 720 K: (a) before irradiation, (b) after 30 s of irradiation, (c) after 720 s

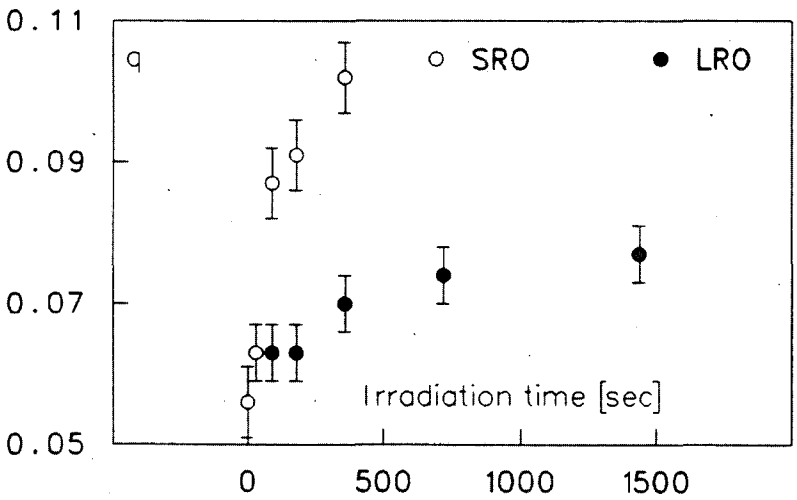

Fig. 10. Cu 20% Pd at 720 K: q vs. irradiation time

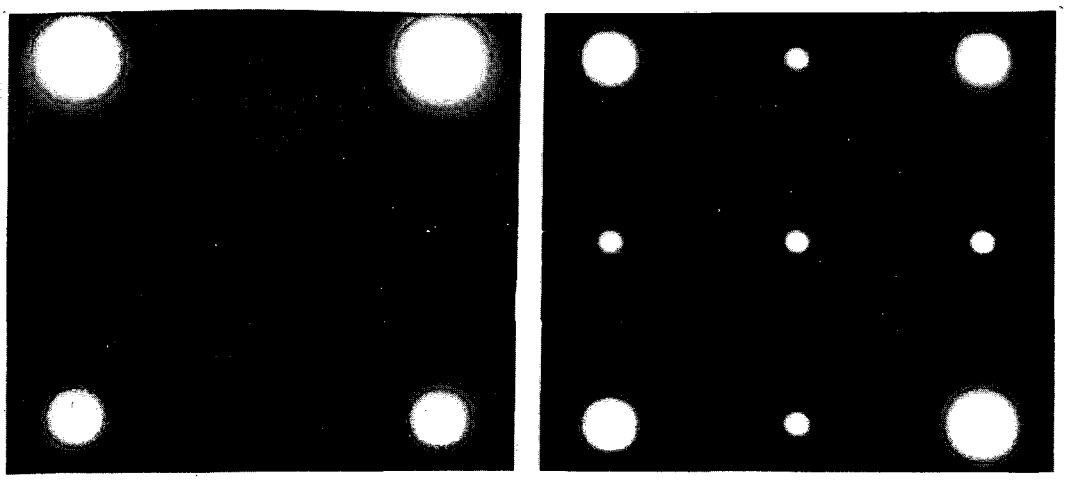

XBB 850-8128

(a) (b)

Fig. 11. Cu 16% Pd: steady states at (a) room temperature and (b) 520 K

is detectable in the intensity at the [100] or [110] positions. If any satellites are present, their separation must be very small as may be seen by extrapolating the data of OHSHIMA and WATANABE [21] or the calculated values of GYORFFY and STOCKS [18]. The as-quenched specimen was disordered, as was the 20% specimen, at 90 K, and the temperature was then increased to room temperature whereupon, after prolonged irradiation, the spots are sufficiently intense to show clearly that no long wavelength modulation is present. Similarly, at 520 K and at 670 K no modulation is present. Figure 11 shows the steady states at room temperature and at 520 K.

For the 18% Pd specimen, destruction of SRO at 90 K followed by irradiation at room temperature results in the modulated SRO state with q smaller than that at 20%. Similarly, modulated SRO persists at 480 K (Fig. 12(a)). At 630 K, however, sharp superstructure peaks appear only at the <100> positions, as seen in Fig. 12(b), indicating *unmodulated* LRO, the $L1_2$ structure, which is the expected equilibrium structure at this temperature. However, room temperature irradiation of the LRO $L1_2$ structure (which had been obtained by a furnace anneal at 623 K) did not result in modulated SRO. The superlattice peaks became broad and diffuse but maintained their spherical symmetry. This observation agrees with the interpretation of the modulated SRO as being spinodally developed since it appears that the system must first be in the disordered state before the modulated SRO appears. (See the discussion of spinodal ordering below.)

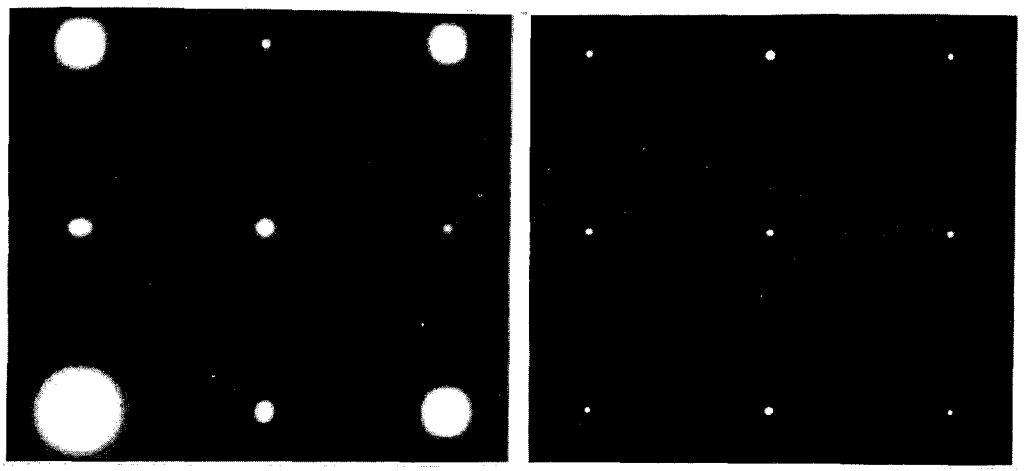

XBB 850-8127

(a) (b)

Fig. 12. Cu 18% Pd: steady states at (a) 480 K and (b) 630 K

For specimens of 22 and 26% Pd, the general tendencies are the same as those of the 20% Pd specimen. Modulated SRO persists at room temperature with the satellite spacing becoming progressively larger as the Pd content increases, while at sufficiently high temperatures the one-dimensional LPS develops. The two-dimensional LPS, expected at 26% Pd, was not observed. This may be due to insufficient time to allow nucleation of this phase.

Before proceeding to the next section to discuss the theory of spinodal ordering, we remark on the possibility that local compositional changes may occur in a specimen as a result of irradiation by a strongly focused high energy electron beam. Calculations have demonstrated the possibility of this phenomenon [26], and there is some experimental evidence for it as well [27]. We attempted to detect such a possible change of local composition using energy dispersive x-ray analysis. A specimen irradiated in the HVEM was transferred to a JEOL JEM 200CX analytical microscope equipped with an energy dispersive x-ray detector. No change of composition in the irradiated regions was detected, although it is possible that such a change would be below the

detectability of such a system which is accurate to about 1%. In this regard, we note that the modulation wave vector of the 22% and 26% specimens does not change under irradiation at room temperature whereas those at 18% and 20% do change. A possible explanation for the change of wave vector in the 18 and 20% specimens is, of course, a local beam induced composition change. However, the lack of change with time in the 22 and 26% specimens argues against the occurrence of a composition change. It seems reasonable to assume that if a local composition change occurs it should do so for all of our specimens. Therefore, we suggest that the change in modulation wave vector in the 18% and 20% specimens is a real thermodynamic effect (possibly induced by the electron beam) and *not* the result of a composition change. Since the rate of change of q with respect to c is approximately constant from about 17 to 30% Pd, one would expect to see a change in wave vector in all the samples under irradiation provided that any possible composition change is of the same order of magnitude for all specimens. (The near constancy of $\partial q/\partial c$ can be deduced from previously published data such as that of OHSHIMA and WATANABE [21].)

3. Theory and Discussion

The present results are explainable, in part, in terms of the phenomenon of spinodal ordering. The theory of spinodal ordering as developed by DE FONTAINE [28, 29] is a theory of early stage kinetics in an unstable disordered solid solution. It should, in a phenomenological sense, explain why, for example, the unstable disordered solid solution of Cu 20% Pd initially evolves toward *modulated* SRO in a region of the phase diagram where the equilibrium ordering wave vector is an *unmodulated* one, i.e., the special point <100>.

The theory of spinodal ordering was originally developed to explain the appearance of peaks of diffuse intensity in rapidly quenched ordering systems [28]. This phenomenon is understood most easily in reciprocal space where the configuration of the alloy is described by a set of concentration waves [30-32]. To begin, one writes the configurational free energy in terms of local concentration deviations

$$\gamma(\mathbf{p}) = c(\mathbf{p}) - \bar{c},$$

where $c(\mathbf{p})$ is a suitably averaged concentration at lattice point $\mathbf{p}$ and $\bar{c}$ is the average concentration of the alloy. The free energy is written as an expansion in powers of the $\gamma(\mathbf{p})$:

$$F(\gamma(\mathbf{p}_1), \gamma(\mathbf{p}_2), \cdots, \gamma(\mathbf{p}_N)) = F_0 + F_1 + F_2 + F_3 + \ldots,$$

where N is the number of lattice sites. The terms F_n are given by

$$F_n = \frac{1}{n!}\left[\sum_{\mathbf{p}} \gamma(\mathbf{p}) \frac{\partial}{\partial \gamma(\mathbf{p})}\right]_0^n F, \tag{1}$$

where the subscript 0 indicates that the derivatives are to be evaluated in the disordered state. Since the disordered state corresponds either to a minimum of F (stable or metastable) or to a saddle point (unstable), then $F_1 = 0$. So we can say

$$\Delta F \equiv F - F_0 = F_2 + F_3 + F_4 + \ldots,$$

where ΔF is the difference in free energies between a given state (described by the set $\{\gamma(\mathbf{p})\}$ for all $\mathbf{p}$) and the completely disordered state. In Fourier space, the preceding expansion contains terms like the following:

$$F_2 = \frac{N}{2}\sum_{\mathbf{k}} f_2(\mathbf{k}) \, |\Gamma(\mathbf{k})|^2,$$

$$F_3 = \frac{N}{3!} \sum_{\mathbf{k}_1,\mathbf{k}_2,\mathbf{k}_3} f_3(\mathbf{k}_1, \mathbf{k}_2, \mathbf{k}_3) \Gamma(\mathbf{k}_1) \Gamma(\mathbf{k}_2) \Gamma(\mathbf{k}_3) \delta(\mathbf{k}_1 + \mathbf{k}_2 + \mathbf{k}_3 - \mathbf{g}), \tag{2}$$

where the $\{\Gamma(\mathbf{k})\}$ are the Fourier transforms of the $\{\gamma(\mathbf{p})\}$. In other words, $\Gamma(\mathbf{k})$ is the amplitude

of the concentration wave of wave vector $\mathbf{k}$. The quantities $f_2(\mathbf{k})$ and $f_3(\mathbf{k}_1,\mathbf{k}_2,\mathbf{k}_3)$ are the Fourier transforms of the second and third derivatives, i.e., the derivatives that arise in the expansion as given in (1). For the third order term, if the three wave vectors $\mathbf{k}_1$, $\mathbf{k}_2$, and $\mathbf{k}_3$ sum to a reciprocal lattice vector $\mathbf{g}$, then the Kronecker delta in (2) equals unity.

It is the term F_2 which will interest us here. According to Landau theory, a second order transition occurs when $f_2(\mathbf{k})$ changes sign for the particular wave vector $\mathbf{k}^0$ at which $f_2(\mathbf{k})$ is a minimum. The temperature for the second order transition is then determined by the condition

$$f_2(\mathbf{k}^0, c, T) = 0, \tag{3}$$

where we have indicated that f_2, in addition to being a function of $\mathbf{k}$, depends on the concentration c and the temperature T. Equation (3) then defines a critical temperature $T_0(c)$ for each concentration c.

The system of interest here, Cu-Pd, undergoes not a second order transition but rather a first order one. In this case, one or more concentration waves combine to give negative contributions to some of the higher order terms $F_3, F_4, \ldots$ in the expansion. Thus, ΔF can change sign at some temperature $T_t > T_0$. In this case, T_0 is no longer a transition temperature but an instability, or *spinodal*, temperature below which the disordered state is unstable with respect to the spontaneous growth of concentration waves with wave vectors $\mathbf{k}^0$ and those obtained from $\mathbf{k}^0$ by the point group symmetry operations of the reciprocal lattice [28, 29]. This growth of concentration waves is what has occurred, for example, in the Cu-Pd specimens quenched from 1270 K. More significantly, it is this same phenomenon which was observed *in situ* in the specimens which had been disordered at 90 K and heated to room temperature where the kinetics (enhanced by the electron beam) allowed the development of the SRO state. This same explanation has also been successfully applied to the growth of the SRO state in irradiated Ni_4Mo [23-25]. That the SRO state below T_0 is qualitatively similar to the fluctuating state above T_t follows because in both cases it is the second order term in the free energy expansion which governs the configuration of the alloy. The SRO state below T_0 is energetically favorable provided the concentration wave amplitudes remain small. (Of course, higher order terms must prevent the unlimited growth of the concentration waves.) Likewise, above T_t the fluctuations in the alloy as measured by the diffracted intensity of x-rays, for example, are described by the fluctuation-dissipation theorem [29]:

$$I_{SRO}(\mathbf{k}) \propto \frac{k_B T}{f_2(\mathbf{k})}.$$

If one uses a Bragg-Williams (mean field) approximation to obtain a form for $f_2(\mathbf{k})$, one obtains the Krivoglaz-Clapp-Moss formula [31, 33].

The quantity $f_2(\mathbf{k})$ must exhibit the symmetry of the f.c.c. lattice and, consequently, must have extrema at certain special points, namely, <000>, <100>, <1$\frac{1}{2}$0> and <$\frac{1}{2}\frac{1}{2}\frac{1}{2}$> [28]. Often, the absolute minimum of $f_2(\mathbf{k})$ will be at one of these special points as it is, for example, in Ni_4Mo [23-25]. What distinguishes Cu-Pd in this regard is that for Pd content greater than about 16% $f_2(\mathbf{k})$ presents minima *away* from the special point [100] in the Brillouin zone; it is at the [q 10] and equivalent positions that the diffuse intensity appears as the disordered state evolves into the SRO state. In analogy to the definition of a Lifshitz point in modulated systems with second order transitions [32], we can define and attempt to locate a *metastable* Lifshitz point [16, 34]. Such a point is defined as follows: the metastable Lifshitz point L divides an ordering instability (spinodal) line into two segments on one of which the instability occurs at a special point (the [100] point in this example) and on the second of which the instability occurs at a wave vector $\mathbf{k}$ whose coordinates (in this example, [q 10]) vary as some other system parameter (concentration) is varied. The point L is also the terminus of a second line which separates the phase diagram into two regions, one in which f_2 is minimized at the special point corresponding to the previously mentioned spinodal (i.e., [100] in this case) and the second in which f_2 is minimized at

a point removed from the special point by some vector $\mathbf{q}$ (in this case $\mathbf{q} = [q\,00]$). In the Bragg-Williams approximation this second line must be vertical.

Any $\mathbf{k}$-space function such as $f_2(\mathbf{k}, c, T)$ having the required f.c.c. symmetry can be expanded in a sum of "shell functions" (one for each coordination shell). At the point $\mathbf{k} = [q\,10]$, for arbitrary q, if we make the definition

$$f_2(\mathbf{k}, c, T)\,|_{\mathbf{k}=[q\,10]} \equiv \Phi(q, c, T),$$

this expansion reduces to the following cosine series [35]:

$$\Phi(q, c, T) = \omega_0(c, T) + \sum_n \omega_n(c, T) \cos 2\pi n q. \tag{4}$$

In a Bragg-Williams approximation, the ω_n would be independent of T. Note that if the series is truncated at $n = 2$, one has the f.c.c. ordering analog of the ANNNI model. A reasonable model for Cu-Pd, however, would likely require terms beyond $n = 2$ [11, 15].

From (4), it is apparent that if we expand $\Phi(q, c, T)$ in a Taylor series about $q = 0$, only even powers of q appear:

$$\Phi(q, c, T) = \Phi_0 + \Phi_2 q^2 + \Phi_4 q^4 + \ldots \tag{5}$$

The Φ_n in (5) are linear combinations of the ω_n appearing in (4). It was shown elsewhere [13] that Φ_4 will most likely be positive so that when examining (5) one can neglect terms of order 6 and higher. (The expansion is uninteresting, of course, unless Φ_2 changes sign as c is varied.) Recall that the instability occurs when the minimum of f_2 changes sign. The minima of $\Phi(q, c, T)$ are at

$$q = 0 \qquad \text{for } \Phi_2 > 0,$$

$$q = \pm\sqrt{-\Phi_2/2\Phi_4} \quad \text{for } \Phi_2 < 0.$$

The values of Φ at these points are

$$\Phi_{\min}(c, T) = \begin{cases} \Phi_0 & \text{for } \Phi_2 > 0. \\ \Phi_0 - \frac{1}{4}\dfrac{\Phi_2^2}{\Phi_4} & \text{for } \Phi_2 < 0. \end{cases}$$

Thus the spinodal lines in the (c, T) plane on either side of the metastable Lifshitz point L are given by the conditions $\Phi_0 = 0$ for for the special point instability and $\Phi_2^2 - 4\Phi_0\Phi_4 = 0$ for the non-special point instability. The second of these two equations is valid only in the vicinity of the metastable Lifshitz point. In general, we can write simply $\Phi_{\min} = 0$ as the condition which determines the instability. Point L then has coordinates (c_L, T_L) determined by

$$\Phi_0(c_L, T_L) = \Phi_2(c_L, T_L) = 0,$$

which is the intersection of the special point spinodal and the non-special point spinodal.

Figure 1 shows estimates for the three metastable loci,

$$\Phi_0 = 0,$$

$$\Phi_{\min} = 0 \quad \text{for } \Phi_2 < 0,$$

$$\Phi_2 = 0,$$

indicated as dashed lines. The metastable Lifshitz point has been labeled as L. The loci have been drawn in a manner which best accounts for the available data and which is consistent with general theoretical knowledge of alloy phase diagrams and instabilities. The most significant result of the present data is the position of the $\Phi_2 = 0$ instability which is rather far to the left of the two phase region which separates the α' and α_1 phases. The present data are lacking in detail since no composition between 16% and 18% Pd was examined, but at room temperature and up to about 520 K this instability must lie at or near 17% Pd since at these temperatures the SRO steady state under irradiation appears to be unmodulated for the 16% composition but modulated for the 18% composition. As mentioned above, for a GBW approximation the Φ_2 line would be vertical. Here, it was drawn curved for the following reasons. At low temperatures (room temperature to about 520 K) its position was estimated as just described. On the other hand, extrapolation of previous data [21] and first principles calculations [18] indicates that high temperature SRO fluctuations remain modulated for concentrations of Pd as low as 16% or even slightly lower, although this conclusion is not clear from the present data. Furthermore, as mentioned previously, we have seen some indication that the value of q at which the instability appears may decrease with decreasing T. Also, CVM calculations for two-dimensional models [36] clearly yield curved Φ_2 lines.

As for the other two instabilities, $\Phi_0 = 0$ and $\Phi_{min} = 0$, they have been drawn close to the equilibrium first order transitions because experimental evidence [10] indicates very narrow two phase regions so that the postulated peritectoids must be close to being critical endpoints through which instability lines must pass [37]. It must be emphasized, however, that the location of instability lines cannot be determined rigorously by experiment because the temperature at which the system becomes unstable to some set of concentration waves must depend upon the past history of the specimen unlike an equilibrium transition which is independent of history. Nevertheless, approximate determination of stability limits is useful in understanding the behavior of quenched or irradiated solid solutions as is clear from the present discussion.

4. Conclusion

We have reported the serendipitous discovery that room temperature irradiation of a completely disordered solid solution could produce steady state modulated SRO for Cu-Pd samples in regions of the phase diagram where only simple $L1_2$ ordering could be found at equilibrium. The authors believe this to be the first observation of its kind ever reported.

This effect could be explained qualitatively by applying spinodal ordering ideas to irradiated systems and by extending the model "beyond the Lifshitz point," i.e., to cases for which the harmonic coefficient f_2 of the free energy possesses minima away from the special points of high symmetry. These generalizations lead to the notion of special point (commensurate) and non-special point (incommensurate) stability limits and of a metastable Lifshitz point.

The experimental portion of this investigation was made possible by use of a high voltage TEM with which it is possible to study, *in situ*, various types of equilibria: (a) high temperature equilibrium SRO fluctuations, (b) equilibrium LRO at various temperatures and (c) steady state SRO under irradiation at low temperatures. In addition, high energy electron irradiation at very low temperatures may be, in some cases, the best (or perhaps only) way to obtain *completely* disordered systems.

Acknowledgements

The authors are grateful to Drs. A. Finel, P. Turchi and G.M. Stocks for helpful conversations. TEM work was performed on the 1.5 MeV microscope at the National Center for Electron Microscopy, Lawrence Berkeley Laboratory. The authors are indebted to Dr. K. Westmacott for his support and interest and to D. Ackland for invaluable technical help. One of us (S.T.) benefited from an MMRD collaborative fellowship. This work was supported by the Director, Office of Energy Research, Office of Basic Energy Sciences, Materials Sciences Division of the U.S. Department of Energy under Contract No. DE-AC03-76SF00098.

References

1. K. Schubert, B. Kiefer, M. Wilkens, R. Haufler: Z. Metallkd. **46**, 692 (1955)
2. M. Hirabayashi, S. Ogawa: J. Phys. Soc. Japan **12**, 259 (1957)
3. K. Okamura: J. Phys. Soc. Japan **28**, 1005 (1970)
4. O. Michikami, H. Iwasaki, S. Ogawa: J. Phys. Soc. Japan **31**, 956 (1971)
5. A. Souter, A. Colson, J. Hertz: Mem. Sci. Rev. Met. **68**, 575 (1971)
6. D. Watanabe, S. Ogawa: J. Phys. Soc. Japan **11**, 226 (1956)
7. M. Guymont, D. Gratias: Phys. stat. sol. (a) **36**, 329 (1976)
8. M. Guymont, R. Portier, D. Gratias: In *Electron Microscopy and Analysis 1981*, ed. by M.J. Goringe, Inst. Phys. Conf. Ser. No. 61 (Inst. Phys., Bristol and London 1981) p. 387
9. O. Terasaki, D. Watanabe: Jpn. J. Appl. Phys. **20**, 1381 (1981)
10. P.R. Subramanian, D.E. Laughlin: Bulletin of Alloy Phase Diagrams (to be published)
11. D. Broddin, G. van Tendeloo, J. van Landuyt, S. Amelinckx, R. Portier, M. Guymont, A. Loiseau: Phil. Mag. **A54**, 395 (1986)
12. J. Kulik, D. de Fontaine: In *Phase Transformations in Solids*, ed. by T. Tsakalakos, Materials Research Society Symposia Proceedings vol. 21 (North-Holland, NY 1984) p. 225
13. D. de Fontaine, J. Kulik: Acta metall. **33**, 145 (1985)
14. A. Loiseau, G. van Tendeloo, R. Portier, F. Ducastelle: J. de Physique **46**, 595 (1985)
15. D. de Fontaine, A. Finel, S. Takeda, J. Kulik: In *Noble Metal Alloys*, ed. by T. B. Massalski, W.B. Pearson, L.H. Bennett and Y.A. Chang (The Metallurgical Society, Inc., Warrendale, PA 1986) p. 49
16. J. Kulik, S. Takeda, D. de Fontaine: Acta metall. **35**, 1137 (1987)
17. H. Sato, R.S. Toth: In *Alloying Behavior and Effects in Concentrated Solid Solutions*, ed. by T.B. Massalski, Metallurgical Society Conferences vol. 29 (Gordon and Breach, NY 1965) p. 295
18. B.L. Gyorffy, G.M. Stocks: Phys. Rev. Letters **50**, 374 (1983)
19. K. Urban, S. Banerjee, J. Mayer: In *Phase Stability and Phase Transformations*, ed. by R. Krishnan, S. Banerjee and P. Mukhopadhyay, Materials Science Forum vol. 3 (Trans Tech Publications, Switzerland 1985) p. 335
20. K. Ohshima, D. Watanabe, J. Harada: Acta Crystallogr. **A32**, 883 (1976)
21. K. Ohshima, D. Watanabe: Acta Crystallogr. **A29**, 520 (1973)
22. G. van Tendeloo, S. Amelinckx: J. de microscopie et de spectroscopie electronique **6**, 371 (1981)
23. S. Banerjee, K. Urban, M. Wilkens: Acta metall. **32**, 299 (1984)
24. S. Banerjee, K. Urban: Phys. stat. sol. (a) **81**, 145 (1984)
25. J. Mayer, K. Urban: Acta metall. (to be published)
26. P.R. Okamoto, N.Q. Lam: In *Advanced Photon and Particle Techniques for the Characterization of Defects in Solids*, ed. by J.B. Roberto, R.W. Carpenter and M.C. Wittels, Mat. Res. Soc. Symposium Proceedings vol. 41 (Materials Research Society, 1985) p. 241
27. N.Q. Lam, G. K. Leaf, M. Minkoff: J. Nucl. Mater. **118**, 248 (1983)
28. D. de Fontaine: Acta metall. **23**, 553 (1975)
29. D. de Fontaine: Solid State Physics **34**, 73 (1979)
30. L.D. Landau, E.M. Lifshitz: *Statistical Physics* (Addison- Wesley, Reading, MA 1958)
31. M.A. Krivoglaz: *The Theory of X-ray and Thermal Neutron Scattering from Real Crystals* (Plenum, NY 1969)
32. A.G. Khachaturyan: Phys. stat. sol. (b) **60**, 9 (1973)
33. P.C. Clapp, S.C. Moss: Phys. Rev. **142**, 418 (1966)
34. R.M. Hornreich, M. Luban, S. Shtrikman: Phys. Rev. **B19**, 3799 (1979)
35. S. Takeda, J. Kulik, D. de Fontaine: Acta metall. (to be published)
36. A. Finel, D. de Fontaine: J. Stat. Physics **43**, 645 (1986)
37. S.M. Allen, J.W. Cahn: In *Alloy Phase Diagrams*, ed. by L.H. Bennett, T.B. Massalski and B.C. Giessen (North Holland, NY 1983) p. 195

LAWRENCE BERKELEY LABORATORY
TECHNICAL INFORMATION DEPARTMENT
UNIVERSITY OF CALIFORNIA
BERKELEY, CALIFORNIA 94720